

Sources of secondary organic aerosols in the Pearl River Delta region in fall: Contributions from the aqueous reactive uptake of dicarbonyls



Nan Li ^{a,b}, Tzung-May Fu ^{c,*}, Junji Cao ^{a,d,**}, Shuncheng Lee ^e, Xiao-Feng Huang ^f,
Ling-Yan He ^f, Kin-Fai Ho ^g, Joshua S. Fu ^h, Yun-Fat Lam ⁱ

^a Key Lab of Aerosol Science & Technology, SKLLQG, Institute of Earth Environment, Chinese Academy of Sciences, Xi'an, China

^b Graduate University of Chinese Academy of Science, Beijing, China

^c Department of Atmospheric and Oceanic Sciences and Laboratory for Climate and Ocean-Atmosphere Studies, School of Physics, Peking University, Beijing, China

^d Institute of Global Environmental Change, Xi'an Jiaotong University, Xi'an, China

^e Department of Civil and Structural Engineering, Research Center for Environmental Technology and Management, The Hong Kong Polytechnic University, Hung Hom, Hong Kong, China

^f Key Laboratory for Urban Habitat Environmental Science and Technology, School of Environment and Energy, Peking University Shenzhen Graduate School, Shenzhen, China

^g School of Public Health and Primary Care, The Chinese University of Hong Kong, Sha Tin, Hong Kong, China

^h Department of Civil and Environmental Engineering, University of Tennessee, Knoxville, TN 37996, USA

ⁱ School of Energy and Environment, City University of Hong Kong, Hong Kong, China

HIGHLIGHTS

- ▶ CMAQ model performance enhanced with addition of dicarbonyl SOA source.
- ▶ 75% of total SOA was biogenic for the PRD in fall and isoprene was the most important precursor.
- ▶ The irreversible uptake of dicarbonyls by aqueous particles was an important SOA formation pathway in the PRD in fall.

ARTICLE INFO

Article history:

Received 10 July 2012

Received in revised form

26 October 2012

Accepted 4 December 2012

Keywords:

Secondary organic aerosol

Glyoxal

Methylglyoxal

CMAQ

Pearl River Delta (PRD)

ABSTRACT

We used the regional air quality model CMAQ to simulate organic aerosol (OA) concentrations over the Pearl River Delta region (PRD) and compared model results to measurements. Our goals were (1) to evaluate the potential contribution of the aqueous reactive uptake of dicarbonyls (glyoxal and methylglyoxal) as a source of secondary organic aerosol (SOA) in an urban environment, and (2) to quantify the sources of SOA in the PRD in fall. We improved the representation of dicarbonyl gas phase chemistry in CMAQ, as well as added SOA formation via the irreversible uptake of dicarbonyls by aqueous aerosols and cloud droplets, characterized by a reactive uptake coefficient $\gamma = 2.9 \times 10^{-3}$ based on laboratory studies. Our model results were compared to aerosol mass spectrometry (AMS) measurements in Shenzhen during a photochemical smog event in fall 2009. Including the new dicarbonyl SOA source in CMAQ led to an increase in the simulated mean SOA concentration at the sampling site from $4.1 \mu\text{g m}^{-3}$ to $9.0 \mu\text{g m}^{-3}$ during the smog event, in better agreement with the mean observed oxygenated OA (OOA) concentration ($8.0 \mu\text{g m}^{-3}$). The simulated SOA reproduced the variability of observed OOA ($r = 0.89$). Moreover, simulated dicarbonyl SOA was highly correlated with simulated sulfate ($r = 0.72$), consistent with the observed high correlation between OOA and sulfate ($r = 0.84$). Including the dicarbonyl SOA source also increased the mean simulated concentrations of total OA from $8.2 \mu\text{g m}^{-3}$ to $13.1 \mu\text{g m}^{-3}$, closer to the mean observed OA concentration ($16.5 \mu\text{g m}^{-3}$). The remaining difference between the observed and simulated OA was largely due to impacts from episodic biomass burning emissions, but the model did not capture this variability. We concluded that, for the PRD in fall and outside of major biomass burning events, 75% of the total SOA was biogenic. Isoprene was the most important precursor,

* Corresponding author.

** Corresponding author. Key Lab of Aerosol Science & Technology, SKLLQG, Institute of Earth Environment, Chinese Academy of Sciences, Xi'an, China.
E-mail addresses: tmfu@pku.edu.cn (T.-M. Fu), cao@loess.llqg.ac.cn (J. Cao).

accounting for 41% of the total SOA. Aromatics accounted for 13% of the total SOA. Our results show that the aqueous chemistry of dicarbonyls can be an important SOA source, potentially accounting for 53% of the total surface SOA in the PRD in fall.

© 2012 Elsevier Ltd. All rights reserved.

1. Introduction

High concentrations of fine particulate matter (PM_{2.5}) are the frequent culprit of poor air quality in the Pearl River Delta region (PRD) of south China (Chan and Yao, 2008). Measurements showed that 30%–40% of PM_{2.5} mass in the PRD is composed of organic material (e.g. Cao et al., 2004; Ho et al., 2006), and up to 80% of that organic aerosol (OA) is secondary (e.g. Cao et al., 2004; Ho et al., 2006; L.-Y. He et al., 2011), i.e. produced in the atmosphere from gaseous organic compounds. Therefore, there is a pressing need to better understand the sources of secondary organic aerosol (SOA) in the PRD, in order to formulate effective air quality control strategies.

Several studies have used regional models to quantify the sources of SOA in the PRD. Han et al. (2008) and Jiang et al. (2012) simulated SOA over China and found 65%–90% of the simulated SOA in southern China to be biogenic, with monoterpenes being the most important precursor. Fu et al. (2012) found 70% of the simulated annual mean surface secondary organic carbon (SOC) in eastern China to be biogenic, but with isoprene as the largest contributor. Wang et al. (2009) found that anthropogenic aromatics account for 55%–65% of the simulated surface SOA in the PRD in spring. However, all of these model studies underestimated surface organic carbon aerosol (OC) concentrations by 30%–60% in the PRD, largely due to an underestimation of the secondary component.

Underestimation of SOA is a major issue in almost all current air quality and atmospheric chemistry models, because the precursors and formation pathways of SOA are not yet well understood (Hallquist et al., 2009). Traditionally, models describe SOA formation as a reversible-partitioning of the semi-volatile oxidation products of volatile organic compounds (VOCs) onto preexisting organic aerosols (Pankow, 1994a, b), with isoprene, terpenes, aromatics, and long alkanes being the VOC precursors based on the laboratory studies. With the exception of Fu et al. (2012), all of the models previously used to investigate the SOA sources in the PRD simulated SOA formation solely via this pathway. Not only do such models underestimate SOA, but they also fail to reproduce the observed variability in SOA, including the frequently observed correlations between SOA and aerosol sulfate (e.g. Yuan et al., 2006; L.-Y. He et al., 2011). This suggests that additional SOA formation pathways, especially one involving the aqueous phase, may be missing from current models.

Aqueous chemistry of glyoxal and methylglyoxal could provide such a pathway. Glyoxal and methylglyoxal are produced during the oxidation of many anthropogenic and biogenic VOCs (Fu et al., 2008; Myriokefalitakis et al., 2008). Laboratory and field studies found rapid production of SOA when these dicarbonyls are in contact with aqueous particles (e.g., Liggio et al., 2005; Volkamer et al., 2009). However, much uncertainties remain with regard to the chemical mechanism, rate, reversibility, and possible acid-catalysis of this SOA source, as well as the eventual fate of the SOA thus produced (e.g. Lim et al., 2010; Ervens et al., 2011). Nevertheless, the potential contribution of a dicarbonyl SOA formation pathway warrants further investigation.

Several model studies have evaluated the potential contribution of dicarbonyl SOA by implementing parameterizations based on different laboratory studies and comparing model results to observations. Using a regional model, Carlton et al. (2008) simulated the OH-oxidation ($k_{\text{OH}} = 3 \times 10^{10} \text{ M}^{-1} \text{ s}^{-1}$) of dissolved

dicarbonyls in cloud and fog water to form non-volatile SOA based on Carlton et al. (2007). They found that including this in-cloud SOA source led to a 30% increase in the simulated OC in the free troposphere over eastern North America in summer of 2004. However, simulation over the entire U.S. showed that this in-cloud SOA source has little contribution to the monthly mean surface OC (Carlton et al., 2010). Fu et al. (2008, 2009, 2012) simulated large global SOA production via the irreversible uptake of dicarbonyls by wet aerosols and cloud droplets, characterized by a reactive uptake coefficient $\gamma = 2.9 \times 10^{-3}$. They showed that including this dicarbonyl SOA source doubled the simulated surface SOA, in better agreement with surface OC observations over eastern North America and over China. However, the enhanced contribution of dicarbonyl SOA relative to total OA in the mid-troposphere predicted by the Fu et al. (2008) model is not supported by aircraft measurements (Heald et al., 2011). To the best of our knowledge, the potential contribution of a dicarbonyl SOA source has not yet been evaluated against high temporal resolution measurements in an urban environment.

In this study, we modified the regional air quality model CMAQ to include the irreversible uptake of dicarbonyls by aqueous particles as a pathway for SOA formation. We used the modified model to simulate OA over the PRD in fall, the season when photochemical smog events occur most frequently in this region (e.g., Zheng et al., 2010), and compared model results against aerosol mass spectrometry (AMS) measurements at a PRD urban site. Our objectives were two-fold: (1) to evaluate the potential contribution of the irreversible uptake of dicarbonyls by aqueous particles as a source of SOA in an urban environment, and (2) to quantify the sources of SOA in the PRD in fall.

2. Model and data

2.1. The CMAQ model

2.1.1. Model setup

We used the 3-D regional air quality model CMAQ (Binkowski and Roselle, 2003) (version 4.7.1) to simulate OA in the PRD in fall. Our CMAQ model was driven by meteorology fields simulated by the Weather Research and Forecasting model (WRF, version 3.2.1) (Skamarock et al., 2008). Fig. 1 shows the three nested domains in our simulation, with horizontal resolutions of 27 km, 9 km, and 3 km, respectively. Vertical layers in our CMAQ simulations (26 layers) extended from the surface to 50 hPa, with 17 layers in the bottom 1 km. Initial and boundary concentrations for the CMAQ simulation were taken from monthly mean concentrations simulated by a global chemical transport model (Fu et al., 2012; Lam and Fu, 2010). Our simulation was initialized for 24 h. Results from 25 October to 7 November 2009 were analyzed.

2.1.2. Modifications to the gas phase chemical mechanism

We modified the SAPRC-99 gas phase chemical mechanism in CMAQ (Carter, 2000a,b; Carlton et al., 2010) to better represent the gas phase chemistry of dicarbonyls. The standard SAPRC-99 represented glyoxal and methylglyoxal as explicit tracers. Primary precursors of the dicarbonyls in the standard SAPRC-99 in CMAQ included isoprene, monoterpenes, propane and acetylene (lumped), ethylene, propene (lumped with >C3 alkenes), benzene, toluene

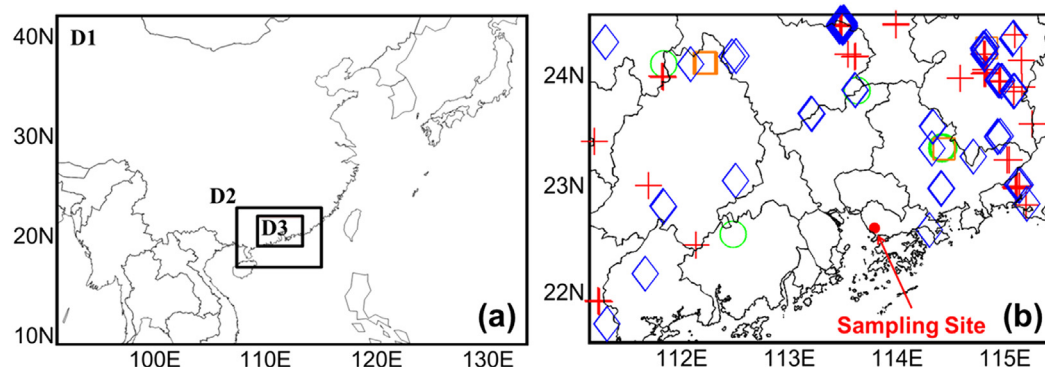


Fig. 1. (a) The three nested domains used in our CMAQ simulation. (b) The inner-most simulation domain. The red dot marks the location of the AMS measurement site (L.-Y. He et al., 2011). The markers indicate fire pixels observed by the MODIS instrument during 25–29 October (circles), 30 October to 1 November (squares), 2 November (crosses), and 3–7 November, 2009 (diamonds). (For interpretation of the references to color in this figure legend, the reader is referred to the web version of this article.)

(lumped with other aromatics with $k_{OH} < 2 \times 10^4 \text{ ppm}^{-1} \text{ min}^{-1}$, excluding benzene), xylenes (lumped with other aromatics with $k_{OH} > 2 \times 10^4 \text{ ppm}^{-1} \text{ min}^{-1}$), phenol, and cresols. Dicarbonyls were removed via the oxidation by OH and NO_3 , as well as photolysis.

Our modifications to the gas phase chemical mechanism largely followed Fu et al. (2008), which was in turn based on the Master Chemistry Mechanism version 3.1 (MCMv3.1) (Saunders et al., 2003). We separated acetylene and propene from their original lumped species and added their explicit dicarbonyl production. We updated the yields of dicarbonyls from aromatic precursors following Carter (2010).

Isoprene is the most important precursor for dicarbonyls, and we made a particular effort to improve the model representation of isoprene chemistry leading to dicarbonyl formation. We added nighttime production of glyoxal from the oxidation of isoprene and propene by NO_3 . Glycolaldehyde and hydroxyacetone are intermediate oxidation products of many VOC species, particularly isoprene. We separated glycolaldehyde and hydroxyacetone from their original lumped tracers and added their production from isoprene, acetone, propene, and ethylene to the chemical mechanism. We added the OH-oxidation of glycolaldehyde and hydroxyacetone (forming glyoxal and methylglyoxal, respectively), as well as NO_3 -oxidation and photolysis (not forming dicarbonyls).

2.1.3. OA in CMAQ and modifications to the SOA formation pathways

OA in the CMAQ model included primary OA (POA) and SOA. The microphysical processes of POA and the various types of SOA were simulated using moment-based parameterizations. All OA were removed by dry and wet deposition.

SOA in the standard CMAQ model included semi-volatile SOA and non-volatile SOA (Carlton et al., 2010). Semi-volatile SOA were produced by the reversible-partitioning of semi-volatile oxidation products from isoprene, monoterpenes, sesquiterpenes, aromatics, and long alkanes, with updated partitioning parameters based on recent laboratory results. All semi-volatile SOA were assumed to oligomerize at a first-order rate $k_{\text{olig}} = 9.6 \times 10^{-6} \text{ s}^{-1}$ to form non-volatile SOA. Acid-enhanced oxidation of isoprene and low- NO_x oxidation of aromatics also formed non-volatile SOA directly.

We turned off the SOA production via in-cloud oxidation of dicarbonyls in CMAQ implemented by Carlton et al. (2008). The SOA thus produced (denoted as AORGC in CMAQ literature) is not additive to the SOA produced via the aqueous irreversible uptake of dicarbonyls that we wished to evaluate in this study, as these parameterizations were based on different assumptions for dicarbonyl aqueous chemistry. In any case, our sensitivity simulation (with updated gas phase chemical mechanism) showed that AORGC accounted for less than 5% of the simulated mean surface SOA over the PRD in fall (Fig. 3a).

We added to the CMAQ model the irreversible aqueous uptake of dicarbonyls by wet aerosols and cloud droplets to form SOA following Fu et al. (2008, 2009). This SOA production was characterized by a reactive uptake coefficient $\gamma = 2.9 \times 10^{-3}$, based on the median experimental results by Liggio et al. (2005) for glyoxal. The same γ value was adopted for methylglyoxal (Zhao et al., 2006). OA water and surface area were calculated following Kim et al. (1993). Cloud droplet surface area was calculated from the WRF-simulated liquid water content in the cloudy fraction of the model grid and by assuming effective droplet radii of $10 \mu\text{m}$ for maritime clouds and $6 \mu\text{m}$ for continental clouds (Heysmsfield, 1993).

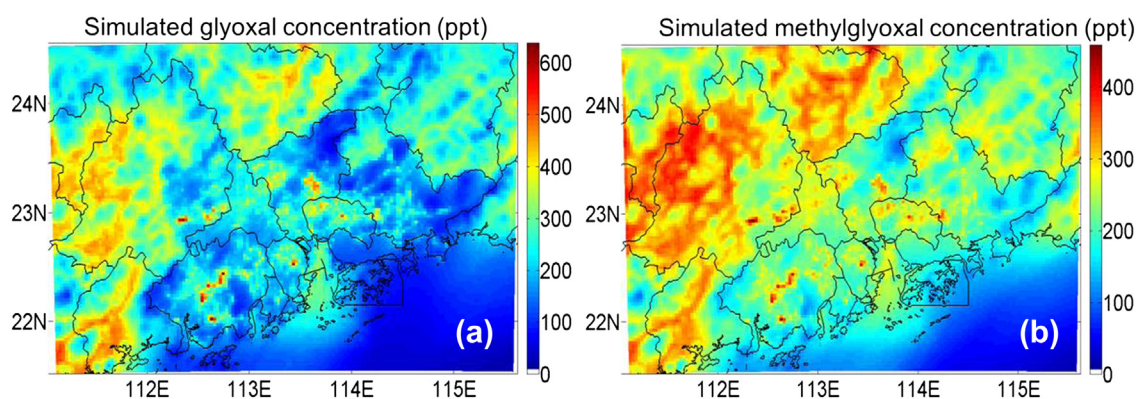


Fig. 2. Mean surface (a) glyoxal and (b) methylglyoxal concentrations simulated by the modified CMAQ model during 25 October to 7 November, 2009.

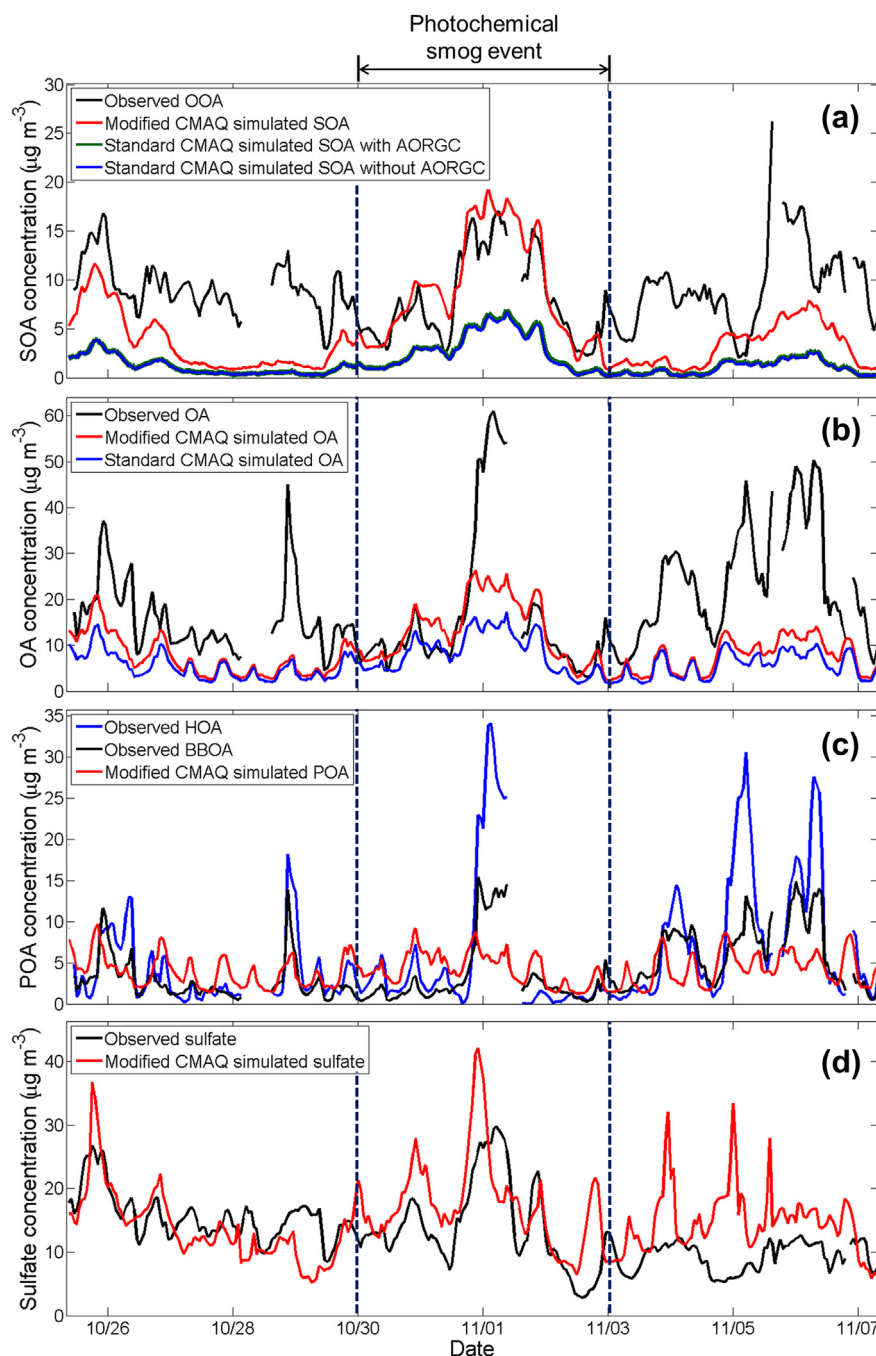


Fig. 3. Simulated and AMS-observed (L.-Y. He et al., 2011) aerosol concentrations at Shenzhen during 25 October to 7 November, 2009. (a) SOA concentrations simulated by the modified CMAQ model (red) and OOA measured by the AMS (black). Also shown are the SOA simulated by the standard CMAQ model with (green) and without (blue) the in-cloud dicarbonyl oxidation SOA (AORGC); the two lines almost entirely overlap. (b) OA simulated by the modified CMAQ model (red) and by the standard CMAQ model (blue), and OA observed by AMS (black). (c) Simulated POA (red), AMS-observed HOA (blue), and AMS-observed BBOA (black). (d) Simulated (red) and observed (black) sulfate. (For interpretation of the references to color in this figure legend, the reader is referred to the web version of this article.)

2.2. Emissions

Anthropogenic emissions of primary OC and non-methane volatile organic compound (NMVOC) precursors were taken from the $0.5^\circ \times 0.5^\circ$ inventory developed by Zhang et al. (2009) for the year 2006. We used a triangle-based technique to linearly interpolate the emission fluxes to the resolutions of our nested domains. For the PRD, anthropogenic OC emission was 39.8 Gg C y^{-1} , with 78.1% from residential activities, 14.1% from industrial activities, 7.8% from transportation, and 0.1% from power generation. Anthropogenic

NMVOC emission for the PRD was 527.2 Gg y^{-1} , mostly from industrial activities (39.6%), and transportation (36.1%), with minor contribution from residential activities (20.1%). We applied seasonal (Zhang et al., 2009) and diurnal variations (Q. Zhang, personal communication, 2011) to Chinese anthropogenic emissions based on provincial statistics. No seasonal or diurnal variations were applied to anthropogenic emissions outside of China. Table S1 summarizes the emission fluxes of dicarbonyl precursors.

Biomass burning emissions of OC and NMVOC precursors for East Asia were from the $1^\circ \times 1^\circ$ inventory developed by Streets et al.

(2003). Biomass burning emissions within the PRD were replaced by the monthly mean inventory developed by M. He et al. (2011) for 2006 with a resolution of 3 km × 3 km. Total OC emitted from biomass burning in the PRD was 9.8 Gg C y⁻¹, including 41% from domestic woody fuel burning, 30% from domestic crop residues burning, 28% from field burning of crop residues, and 1% from forest fire. Biomass burning emits large amounts of glyoxal, methylglyoxal, glycolaldehyde, and hydroxyacetone (Akagi et al., 2011). We estimated these emissions by scaling the biomass burning emissions of CO (Fu et al., 2008).

Biogenic emissions of NMVOC precursors were taken from the Model of Emissions of Gases and Aerosols from Nature (MEGAN) version 2.04 (Guenther et al., 2006). Seasonal and diurnal variation of MEGAN biogenic emissions were driven by meteorological fields simulated by WRF, as well as land cover and leaf area index data from MODIS. Total isoprene and monoterpene emissions from the PRD were 176 Gg y⁻¹ and 149 Gg y⁻¹, respectively.

2.3. AMS observations

We compared our model results to hourly measurements made by L.-Y. He et al. (2011) using an Aerodyne high-resolution time-of-flight AMS in Shenzhen in fall 2009. The sampling site (Fig. 1b and 113.9°E, 22.6°N) was on the western side of Shenzhen City, on the east side of the Pearl River Estuary. Details about the field campaign were given in L.-Y. He et al. (2011). Measurements were conducted from 25 October to 2 December 2009, but we limited our simulation to the period from 25 October to 7 November. The averaged PM₁ mass concentration was 46.3 ± 25.5 μg m⁻³ for the simulated period (44.5 ± 34.0 μg m⁻³ for the entire campaign), with organic matter contributing 40% of the total PM₁ mass.

L.-Y. He et al. (2011) applied positive matrix factorization to the AMS data. They identified four OA components, including hydrocarbon-like OA (HOA), biomass burning OA (BBOA), semi-volatile oxygenated OA (SV-OOA), and low-volatile oxygenated OA (LV-OOA), constituting on average 32%, 23%, 25%, and 20% of the total OA mass during our simulation period, respectively. We used the total oxygenated OA (SV-OOA plus LV-OOA) as a surrogate for SOA for comparison with our simulation.

3. Simulated dicarbonyls in the PRD region

We first examined the dicarbonyls simulated by our modified CMAQ model in the PRD. Previous measurements of dicarbonyl concentrations in urban areas ranged from 25 to 1800 ppt for glyoxal and 22–669 ppt for methylglyoxal, with higher concentrations in summer than in winter (e.g., Grosjean et al., 2002; Volkamer et al., 2005; Possanzini et al., 2007). Our simulated average surface glyoxal and methylglyoxal concentrations over the PRD during 25 October to 7 November 2009 were 212 ppt and 210 ppt, respectively, consistent with previous measurements.

Our simulated glyoxal and methylglyoxal production rate in the PRD were 114 Gg y⁻¹ and 278 Gg y⁻¹, respectively. Isoprene was the single largest contributor to the simulated glyoxal (39%), followed by ethylene (15%), acetylene (15%), xylenes (8%), toluene (7%), and benzene (6%). 43% of the simulated glyoxal was biogenic and 57% was non-biogenic. Isoprene was the dominant source of methylglyoxal (79%), with minor contribution from xylenes (9%). Biogenic and non-biogenic sources accounted 82% and 18% of the simulated methylglyoxal, respectively.

We conducted a simulation using the standard CMAQ model, with the original SAPRC-99 mechanism and the default SOA formation pathways (including AORGC). Using the standard CMAQ model, the simulated glyoxal and methylglyoxal productions in the PRD were 72 Gg y⁻¹ and 180 Gg y⁻¹, respectively, approximately

40% lower than those simulated with our modified CMAQ. A comparison of the dicarbonyl productions simulated by the standard CMAQ and our modified CMAQ is shown in Table S1.

Fig. 2 shows the spatial distributions of surface glyoxal and methylglyoxal concentrations in and around the PRD averaged during 25 October to 7 November 2009, as simulated by our modified CMAQ model. Within the PRD, the surface concentrations of both dicarbonyls generally reflected the spatial distribution of isoprene (Fig. S1a), with superimposed hotspots associated from direct dicarbonyl emissions from biomass burning (Fig. S1c). Outside the PRD, both dicarbonyls showed high surface concentrations over the rural areas in the northwest, north, and southwest, reflecting the biogenic and biomass burning emissions in these areas (Fig. S1).

4. Comparison with AMS measurements

Fig. 3a compares our simulated SOA at the sampling site in Shenzhen with AMS-observed OOA (surrogate for SOA) during 25 October to 7 November 2009. Observed OOA concentrations ranged from 2.0 μg m⁻³ to 26.2 μg m⁻³. Simulated SOA concentrations using the modified CMAQ model ranged from 0.6 μg m⁻³ to 19.2 μg m⁻³. The simulated SOA reproduced the observed OOA concentrations and variability between 30 October and 2 November. However, the model failed to reproduce the observed OOA concentrations and variability from 25 to 29 October and from 3 to 7 November.

We examined the causes for the difference in model performance during these three time periods. Weather maps during the period 25–29 October showed that the pressure gradients were weak over southern China. The observed winds at the sampling site during this period were weak northerlies (Fig. S2). Our WRF simulation reproduced the synoptic scale weather patterns and the low pressure gradients over southern China. However, the simulated winds at the sampling site were weak southerlies, likely because the model failed to capture the local micrometeorology in the absence of strong synoptic weather. As a result, the pollutants from northern PRD were not transported to the sampling site in our CMAQ simulation. Between 3 and 7 November, observed OOA, HOA, and BBOA concentrations were all high and well correlated with one another (Fig. 3). Black carbon, CO, and acetonitrile measurements (not shown) by L.-Y. He et al. (2011) also showed concurrent high concentrations, indicating that the sampling site was heavily impacted by biomass burning emissions. We examined the fire pixel product (MOD14) from the MODIS instrument (Kaufman et al., 2003) during this period and found a large number of fire pixels over the rural areas surrounding the PRD (Fig. 1b). These fires were most likely associated with post-harvest in-field burning of crop residue (M. He et al., 2011). The episodic occurrences and day-to-day changes in location of these fires were not represented in the monthly mean biomass burning inventory we used (M. He et al., 2011).

We focused the discussions below on the period between 30 October and 2 November 2009. Examination of weather maps and satellite images during this period indicated that there was a typhoon (Mirinae) approximately 1200 km south of the PRD. The outflow of that typhoon led to strong subsidence over south China, resulting in high temperature, minimal cloud cover, and compressed boundary layer in the PRD, all favorable conditions for photochemical smog formation. Strong subsidence associated with a nearby typhoon is a typical high pollution scenario for the PRD in fall (e.g. Huang et al., 2009).

Table 1 compares the simulated SOA against the observed OOA at the sampling site during the photochemical smog event. The mean SOA concentration simulated by our modified CMAQ was 9.0 μg m⁻³, in good agreement with the observed OOA concentration (8.0 μg m⁻³). Our simulated SOA also captured the

Table 1

Comparison of simulated and observed OA at Shenzhen during 30 October to 2 November, 2009.

	Measurements ^a		Modified CMAQ		Standard CMAQ	
	OOA	OA	SOA	OA	SOA	OA
Mean concentration ($\mu\text{g m}^{-3}$)	8.0	16.5	9.0	13.1	4.1	8.2
Correlation with observation (r)			0.89 ^b	0.77	0.89 ^b	0.74
Normalized mean bias			14%	–21%	–49%	–51%

^a AMS measurements by L.-Y. He et al. (2011).^b Correlations were calculated against measured OOA.

variability of the observed OOA ($r = 0.89$). We conducted a sensitivity test using the standard CMAQ model. The resulting mean simulated SOA was $4.1 \mu\text{g m}^{-3}$, 49% lower than the observed concentration. The difference in simulated SOA levels between the standard CMAQ model and the modified CMAQ model had little to do with the difference in gas phase dicarbonyl production, since AORGC contributed negligibly to the simulated surface SOA in the standard CMAQ (Fig. 3a). Instead, the significant improvement in the model's ability at reproducing observed OOA was almost entirely due to the inclusion of the aqueous irreversible-uptake dicarbonyl SOA source.

Observed OOA and sulfate were highly correlated ($r = 0.84$) during the photochemical event, suggesting that aqueous processes may be involved during the formation of OOA. Including the irreversible uptake of dicarbonyls by aqueous particles as a source of SOA in the model is consistent with this picture. Fig. 3d shows that our simulation reproduced the observed sulfate concentrations and variability. The correlation between the simulated sulfate and the simulated irreversible-uptake dicarbonyl SOA was 0.72, consistent with the observation. In comparison, the correlation between the simulated sulfate and the simulated non-dicarbonyl SOA was 0.44.

Including the irreversible-uptake dicarbonyl SOA also led to better agreement with the observed total OA. The mean observed OA concentration during the photochemical smog event was $16.5 \mu\text{g m}^{-3}$. The mean OA simulated by the standard CMAQ was $8.2 \mu\text{g m}^{-3}$. Using our modified CMAQ model, the simulated OA was improved to $13.1 \mu\text{g m}^{-3}$. The remaining difference is largely due to a sudden spike in HOA and BBOA between the evening of 31 October and the morning of 1 November, indicating that the sampling site was affected by emissions from biomass burning. As discussed before, these fires were likely associated with post-harvest crop residue burning, but their episodic occurrences were not captured by the emission inventory used in our simulation.

5. SOA sources in the PRD region

The good agreement between our simulated SOA and observed OOA shown in Section 4 lent confidence to our model's capability at quantifying the sources of SOA in the PRD outside of major biomass burning events. Table 2 summarizes the sources of surface SOA in the PRD during the photochemical smog event, as simulated by our modified CMAQ model. Biogenic VOC precursors accounted for 75% of the total simulated SOA. For the biogenic SOA, 26% existed as semi-volatile species in the particulate phase, 29% existed as non-volatile species formed by the oligomerization of the semi-volatile species; 45% was produced via the irreversible uptake of dicarbonyls by aqueous particles (15% from glyoxal and 30% from methylglyoxal). Overall, biogenic isoprene accounted for 41% of the total SOA in the PRD in fall.

Non-biogenic VOC precursors accounted for 25% of total SOA in the PRD in fall. 7% of the non-biogenic SOA existed as semi-volatile species and 16% existed as non-volatile oligomers; 77% of the non-biogenic SOA were produced via the aqueous irreversible-dicarbonyl-uptake pathway (57% from glyoxal and 20% from

methylglyoxal). Aromatics from anthropogenic and biomass burning emissions accounted for 13% of the simulated surface SOA.

Our analyses showed that the irreversible uptake of dicarbonyls by wet aerosols and cloud droplets may be an important source of SOA, potentially accounting for 53% of the simulated surface SOA in the PRD in fall. This is consistent with previous measurement and modeling studies that highlighted the importance of in-cloud processing for SOA formation in the PRD (e.g., Yuan et al., 2006; Huang et al., 2011).

We compared our findings regarding SOA sources in the PRD in fall against results from previous measurement studies. Hu et al. (2008) found that 80%–90% of summertime SOA in Hong Kong was biogenic, but they found much larger contributions from monoterpenes and β -caryophyllene than from isoprene. This may be due to their samples being collected in Hong Kong in Summer, where/when emissions of monoterpenes and β -caryophyllene are stronger. Ding et al. (2012) found aromatics to be the dominant source of the identified SOC in central PRD in summer, fall, and winter. Both Hu et al. (2008) and Ding et al. (2012) were based on SOA chemical tracer analyses. A major uncertainty in such analyses is that the ratio of a specific chemical tracer mass relative to total SOA (or SOC) mass is assumed constant, which may not be valid under all conditions (e.g., low- or high- NO_x , at low or high OA concentrations and acidity) (Hallquist et al., 2009). Hu et al. (2010) and Ding et al. (2012) pointed out that biomass burning emissions contributed significantly to SOA in the PRD. We also found this to be

Table 2

SOA composition in the PRD simulated by the modified CMAQ model during 30 October to 2 November, 2009.

Precursor	Simulated SOA concentrations in the modified CMAQ model ($\mu\text{g m}^{-3}$) ^b				
	Semi-volatile	Non-volatile oligomers	Irreversible-uptake	Irreversible-uptake glyoxal	Total
Biogenic					
Isoprene	0.28	0.55	0.91	2.00	3.74
Monoterpenes	1.50	1.43	0.04	0.02	2.99
Ethylene	.	.	0.06	.	0.06
Acetone	.	.	.	0.04	0.04
Sesquiterpenes	<0.01	<0.01	.	.	<0.01
Non-biogenic					
Xylene	0.05	0.14	0.20	0.23	0.62
Acetylene	.	.	0.35	.	0.35
Toluene	0.03	0.08	0.16	0.07	0.34
Ethylene	.	.	0.30	.	0.30
Benzene	0.02	0.06	0.15	.	0.23
Alkanes	0.06	0.09	.	.	0.15
Glyoxal ^a	.	.	0.12	.	0.12
Hydroxyacetone ^a	.	.	.	0.06	0.06
Methylglyoxal ^a	.	.	.	0.03	0.03
Acetone	.	.	.	0.03	0.03
Glycolaldehyde ^a	.	.	0.03	.	0.03
Cresols	.	.	.	0.03	0.03
Phenol	.	.	0.01	.	0.01
Propene	.	.	.	<0.01	<0.01
Total	1.94	2.35	2.33	2.51	9.13

^a Primary emissions from biomass burning.^b '.' not applicable.

the case, although our model was unable to capture the spatio-temporal variability of biomass burning emissions and their full contribution to SOA.

6. Conclusions

We simulated OA concentrations in the PRD and compared model results to AMS measurements, with the goals of evaluating the potential contribution of the irreversible uptake of dicarbonyls by aqueous particles as a source of SOA, as well as quantifying the sources of SOA in the PRD in fall. We made extensive modifications to the SAPRC-99 gas phase chemistry mechanism in the CMAQ model to improve the representation of dicarbonyl chemistry. We added SOA formation via the irreversible uptake of dicarbonyls by aqueous aerosols and cloud droplets, characterized by a reactive uptake coefficient $\gamma = 2.9 \times 10^{-3}$ based on laboratory studies.

Our simulated average surface glyoxal and methylglyoxal concentrations over the PRD during 25 October to 7 November 2009 were 212 ppt and 210 ppt, respectively, consistent with previous measurements. Isoprene was the single largest contributor to the simulated glyoxal (39%) and the dominant precursor of methylglyoxal (79%).

We compared our OA simulation to AMS measurements at an urban site in the PRD during a photochemical smog event (30 October to 2 November) in fall 2009. Our modified CMAQ (including the new dicarbonyl SOA source) reproduced the concentration and variability of observed OOA. The mean SOA simulated by the modified CMAQ model at the sampling site during the smog event was $9.0 \mu\text{g m}^{-3}$, in good agreement with the mean measured OOA concentration ($8.0 \mu\text{g m}^{-3}$). SOA simulated by the modified CMAQ model also reproduced the variability of measured OOA ($r = 0.89$). Simulated dicarbonyl SOA showed high correlation with simulated sulfate ($r = 0.72$), consistent with the observations. Including the dicarbonyl SOA source also improved the agreement with between simulated and observed OA. The remaining difference was largely due to the observed primary OA being heavily impacted by episodic biomass burning emissions, but the model did not capture this variability.

We concluded that, for the PRD region in fall and outside of major biomass burning events, 75% of the total SOA was biogenic. Isoprene was the most important precursor, accounting for 41% of the total SOA. Aromatics accounted for 13% of the total SOA. We showed that the irreversible uptake of dicarbonyls by aqueous particles may be an important pathway for SOA formation, potentially accounting for 53% of the simulated surface SOA.

Acknowledgments

This work was supported by the Research Grants Council of Hong Kong (PolyU5197/05E), the Strategic Priority Research Program of the Chinese Academy of Sciences (XDA05100401), and the National Natural Science Foundation of China (41222035, 40925009). We thank Prof. J.-Y. Zheng for providing the PRD biomass burning emission inventory.

Appendix A. Supplementary data

Supplementary data related to this article can be found at <http://dx.doi.org/10.1016/j.atmosenv.2012.12.005>.

References

Akagi, S.K., Yokelson, R.J., Wiedinmyer, C., Alvarado, M.J., Reid, J.S., Karl, T., Crouse, J.D., Wennberg, P.O., 2011. Emission factors for open and domestic

- biomass burning for use in atmospheric models. *Atmospheric Chemistry and Physics* 11, 4039–4072.
- Binkowski, F.S., Roselle, S.J., 2003. Models-3 Community Multiscale Air Quality (CMAQ) model aerosol component 1. Model description. *Journal of Geophysical Research* 108 (6), 4183.
- Cao, J.J., Lee, S.C., Ho, K.F., Zou, S.C., Fung, K., Li, Y., Watson, J.G., Chow, J.C., 2004. Spatial and seasonal variations of atmospheric organic carbon and elemental carbon in Pearl River Delta Region, China. *Atmospheric Environment* 38, 4447–4456.
- Carlton, A.G., Bhawe, P.V., Napelenok, S.L., Edney, E.O., Sarwar, G., Pinder, R.W., Pouliot, G.A., Houyoux, M., 2008. CMAQ model performance enhanced when in-cloud secondary organic aerosol is included: comparisons of organic carbon predictions with measurements. *Environmental Science & Technology* 42, 8798–8802.
- Carlton, A.G., Bhawe, P.V., Napelenok, S.L., Edney, E.D., Sarwar, G., Pinder, R.W., Pouliot, G.A., Houyoux, M., 2010. Model representation of secondary organic aerosol in CMAQv4.7. *Environmental Science & Technology* 44, 8553–8560.
- Carlton, A.G., Turpin, B.J., Altieri, K.E., Seitzinger, S., Reff, A., Lin, H.-J., Ervens, B., 2007. Atmospheric oxalic acid and SOA production from glyoxal: results of aqueous photooxidation experiments. *Atmospheric Environment* 41, 7588–7602.
- Carter, W.P.L., 2000a. Documentation of the SAPRC-99 Chemical Mechanism for VOC Reactivity Assessment. Report to the California Air Resources Board, Contracts 92–329 and 95–308.
- Carter, W.P.L., 2000b. Implementation of the SAPRC-99 Chemical Mechanism into the Models-3 Framework. Report to the United States Environmental Protection Agency.
- Carter, W.P.L., 2010. Development of the SAPRC-07 chemical mechanism. *Atmospheric Environment* 44, 5324–5335.
- Chan, C.K., Yao, X.H., 2008. Air pollution in mega cities in China. *Atmospheric Environment* 42, 1–42.
- Ding, X., Wang, X.M., Gao, B., Fu, X.X., He, Q.-F., Zhao, X.Y., Yu, J.Z., Zheng, M., 2012. Tracer-based estimation of secondary organic carbon in the Pearl River Delta, south China. *Journal of Geophysical Research* 117, D05313.
- Ervens, B., Turpin, B.J., Weber, R.J., 2011. Secondary organic aerosol formation in cloud droplets and aqueous particles (aqSOA): a review of laboratory, field and model studies. *Atmospheric Chemistry and Physics* 11, 11069–11102.
- Fu, T.-M., Jacob, D.J., Wittrock, F., Burrows, J.P., Vrekoussis, M., Henze, D.K., 2008. Global budgets of atmospheric glyoxal and methylglyoxal, and implications for formation of secondary organic aerosols. *Journal of Geophysical Research* 113, D15303.
- Fu, T.-M., Jacob, D.J., Heald, C.L., 2009. Aqueous-phase reactive uptake of dicarbonyls as a source of organic aerosol over eastern North America. *Atmospheric Environment* 43, 1814–1822.
- Fu, T.-M., Cao, J.J., Zhang, X.Y., Lee, S.C., Zhang, Q., Han, Y.M., Qu, W.J., Han, Z., Zhang, R., Wang, Y.X., Chen, D., Henze, D.K., 2012. Carbonaceous aerosols in China: top-down constraints on primary sources and estimation of secondary contribution. *Atmospheric Chemistry and Physics* 12, 2725–2746.
- Grosjean, D., Grosjean, E., Moreira, L.F.R., 2002. Speciated Ambient Carbonyls in Rio de Janeiro, Brazil. *Environmental Science & Technology* 36, 1389–1395.
- Guenther, A., Karl, T., Harley, P., Wiedinmyer, C., Palmer, P.L., Geron, C., 2006. Estimates of global terrestrial isoprene emissions using MEGAN (Model of Emissions of Gases and Aerosols from Nature). *Atmospheric Chemistry and Physics* 6, 3181–3210.
- Hallquist, M., Wenger, J.C., Baltensperger, U., Rudich, Y., Simpson, D., Claeys, M., Dommen, J., Donahue, N.M., George, C., Goldstein, A.H., Hamilton, J.F., Herrmann, H., Hoffmann, T., Iinuma, Y., Jang, M., Jenkin, M.E., Jimenez, J.L., Kiendler-Scharr, A., Maenhaut, W., McFiggans, G., Mentel, Th.F., Monod, A., Prévôt, A.S.H., Seinfeld, J.H., Surratt, J.D., Szmigielski, R., Wildt, J., 2009. The formation, properties and impact of secondary organic aerosol: current and emerging issues. *Atmospheric Chemistry and Physics* 9, 5155–5236.
- Han, Z.W., Zhang, R.J., Wang, Q.G., Wang, W., Cao, J.J., Xu, J., 2008. Regional modeling of organic aerosols over China in summertime. *Journal of Geophysical Research* 113, D11202.
- He, L.-Y., Huang, X.-F., Xue, L., Hu, M., Zheng, J., Zhang, R.Y., Zhang, Y.H., 2011. Submicron aerosol analysis and organic source apportionment in an urban atmosphere in Pearl River Delta of China using high-resolution aerosol mass spectrometry. *Journal of Geophysical Research* 116, D12304.
- He, M., Zheng, J.Y., Yin, S.S., Zhang, Y.Y., 2011. Trends, temporal and spatial characteristics, and uncertain ties in biomass burning emissions in the Pearl River Delta, China. *Atmospheric Environment* 45, 4051–4059.
- Heald, C.L., Coe, H., Jimenez, J.L., Weber, R.J., Bahreini, R., Middlebrook, A.M., Russell, L.M., Jolleys, M., Fu, T.-M., Allan, J.D., Bower, K.N., Capes, G., Crosier, J., Morgan, W.T., Robinson, N.H., Williams, P.I., Cubison, M.J., DeCarlo, P.F., Dunlea, E.J., 2011. Exploring the vertical profile of atmospheric organic aerosol: comparing 17 aircraft field campaigns with a global model. *Atmospheric Chemistry and Physics* 11, 12673–12696.
- Heymsfield, A.J., 1993. Microphysical structures of stratiform and cirrus clouds. In: Hobbs, P.V. (Ed.), *Aerosol–Cloud–Climate Interactions*. Academic Press, San Diego, pp. 97–121.
- Ho, K.F., Lee, S.C., Cao, J.J., Li, Y.S., Chow, J.C., Watson, J.G., Fung, K., 2006. Variability of organic and elemental carbon, water soluble organic carbon, and isotopes in Hong Kong. *Atmospheric Chemistry and Physics* 6, 4569–4576.
- Hu, D., Bian, Q.J., Li, T.W.Y., Lau, A.K.H., Yu, J.Z., 2008. Contributions of isoprene, monoterpenes, b-caryophyllene, and toluene to secondary organic aerosols in Hong Kong during the summer of 2006. *Journal of Geophysical Research* 113, D22206.

- Hu, D., Bian, Q., Lau, A.K.H., Yu, J.Z., 2010. Source apportioning of primary and secondary organic carbon in summer PM_{2.5} in Hong Kong using positive matrix factorization of secondary and primary organic tracer data. *Journal of Geophysical Research* 115, D16204.
- Huang, X.H.H., Ip, H.S.S., Yu, J.Z., 2011. Secondary organic aerosol formation from ethylene in the urban atmosphere of Hong Kong: a multiphase chemical modeling study. *Journal of Geophysical Research* 116, D03206.
- Huang, X.-F., Yu, J.Z., Yuan, Z.B., Lau, A.K.H., Louie, P.K.K., 2009. Source analysis of high particulate matter days in Hong Kong. *Atmospheric Environment* 43, 1196–1203.
- Jiang, F., Liu, Q., Huang, X.X., Wang, T.J., Zhuang, B.L., Xie, M., 2012. Regional modeling of secondary organic aerosol over China using WRF/Chem. *Journal of Aerosol Science* 43, 57–73.
- Kaufman, Y., Ichoku, C., Giglio, L., Korontzi, S., Chu, D., Hao, W., Li, R., Justice, C., 2003. Fire and smoke observed from the Earth Observing System MODIS instrument-products, validation, and operational use. *International Journal of Remote Sensing* 24 (8), 1765–1781.
- Kim, Y.P., Seinfeld, J.H., Saxena, P., 1993. Atmospheric gas-aerosol equilibrium, I. Thermodynamic model. *Aerosol Science and Technology* 19, 157–181.
- Lam, Y.F., Fu, J.S., 2010. A novel downscaling technique for the linkage of global and regional air quality modeling. *Atmospheric Chemistry and Physics* 10, 4013–4031.
- Liggio, J., Li, S.-M., McLaren, R., 2005. Reactive uptake of glyoxal by particulate matter. *Journal of Geophysical Research* 110, D10304.
- Lim, Y.B., Tan, Y., Perri, M.J., Seitzinger, S.P., Turpin, B.J., 2010. Aqueous chemistry and its role in secondary organic aerosol (SOA) formation. *Atmospheric Chemistry and Physics* 10, 10521–10539.
- Myriokefalitakis, S., Vrekoussis, M., Tsigaridis, K., Wittrock, F., Richter, A., Brüehl, C., Volkamer, R., Burrows, J.P., Kanakidou, M., 2008. The influence of natural and anthropogenic secondary sources on the glyoxal global distribution. *Atmospheric Chemistry and Physics* 8, 4965–4981.
- Pankow, J.F., 1994a. An absorption model of gas/particle partitioning of organic compounds in the atmosphere. *Atmospheric Environment* 28, 185–188.
- Pankow, J.F., 1994b. An absorption model of gas/particle partitioning involved in the formation of secondary organic aerosol. *Atmospheric Environment* 28, 189–193.
- Possanzini, M., Tagliacozzo, G., Cecinato, A., 2007. Ambient levels and sources of lower carbonyls at Montelibretti, Rome (Italy). *Water Air and Soil Pollution* 183, 447–454.
- Saunders, S.M., Jenkin, M.E., Derwent, R.G., Pilling, M.J., 2003. Protocol for the development of the Master Chemical Mechanism, MCMv3 (Part A): tropospheric degradation of non-aromatic volatile organic compounds. *Atmospheric Chemistry and Physics* 3, 161–180.
- Skamarock, W.C., Klemp, J.B., Dudhia, J., Gill, D.O., Barker, D.M., Duda, M.G., Huang, X.-Y., Wang, W., Powers, J.G., 2008. A Description of the Advanced Research WRF Version 3. NCAR Tech Notes-475+STR.
- Streets, D.G., Yarber, K.F., Woo, J.H., Carmichael, G.R., 2003. Biomass burning in Asia: annual and seasonal estimates and atmospheric emissions. *Global Biogeochemical Cycles* 17, 1099.
- Volkamer, R., Molina, L.T., Molina, M.J., 2005. DOAS measurement of glyoxal as an indicator for fast VOC chemistry in urban air. *Geophysical Research Letters* 32, L08806.
- Volkamer, R., Ziemann, P.J., Molina, M.J., 2009. Secondary Organic Aerosol Formation from Acetylene (C₂H₂): seed effect on SOA yields due to organic photochemistry in the aerosol aqueous phase. *Atmospheric Chemistry and Physics* 9, 1907–1928.
- Wang, X.M., Wu, Z.Y., Liang, G.X., 2009. WRF/CHEM modeling of impacts of weather conditions modified by urban expansion on secondary organic aerosol formation over Pearl River Delta. *Particuology* 7, 384–391.
- Yuan, Z.B., Yu, J.Z., Lau, A.K.H., Louie, P.K.K., Fung, J.C.H., 2006. Application of positive matrix factorization in estimating aerosol secondary organic carbon in Hong Kong and its relationship with secondary sulfate. *Atmospheric Chemistry and Physics* 6, 25–34.
- Zhang, Q., Streets, D.G., Carmichael, G.R., He, K.B., Huo, H., Kannari, A., Klimont, Z., Park, I.S., Reddy, S., Fu, J.S., Chen, D., Duan, L., Lei, Y., Wang, L.T., Yao, Z.L., 2009. Asian emissions in 2006 for the NASA INTEX-B mission. *Atmospheric Chemistry and Physics* 9, 5131–5153.
- Zhao, J., Levitt, N.P., Zhang, R.Y., Chen, J.M., 2006. Heterogeneous reactions of methylglyoxal in acidic media: implications for secondary organic aerosol formation. *Environmental Science and Technology* 40, 7682–7687.
- Zheng, J.Y., Zhong, L.J., Wang, T., Louie, P.K.K., Li, Z.C., 2010. Ground-level ozone in the Pearl River Delta region: analysis of data from a recently established regional air quality monitoring network. *Atmospheric Environment* 44, 814–823.